

Finely-tuned strength-toughness balance of PPR/UHMWPE blends via shear-enhanced crystal orientation and cocrystal-locked UHMWPE particles

Zhijie Zhao^{1,2,3,4,*}, Ping Hai^{1,2,3,4,*}, Minjuan Zhang^{1,2,3,4}, Yongbiao Zheng^{1,2,3,4}, Yuerong Chen^{1,2,3,4}, Cunling Long^{1,2,3,4}, Hongtao Zhang^{1,2,3,4}, Xinyi Zhang^{1,2,3,4}

¹Qinghai Provincial Drug inspection and Testing Institute, Xi'ning, 810016, China

²Qinghai Provincial Key laboratory of Modernization of Traditional Chinese and Tibetan Medicine, Xi'ning, 810016, China

³Qinghai Institute of Medical Device Supervision and Testing, Xi'ning, 810016, China

⁴NMPA Key Laboratory for Quality Control of TCM (Tibetan Medicine), Xi'ning, 810016, China

*Corresponding Authors: Zhijie Zhao: zhijiezhao@yeah.net

Ping Hai: 352786498@qq.com

Received: 11 April 2024, Accepted: 6 July 2024

DOI: 10.22063/POJ.2024.3605.1303

ABSTRACT

The presence of ultrahigh molecular weight species in polymer melt facilitates the formation of highly-oriented crystalline structures and favors the improvement of mechanical properties. However, due to the random copolymer chain architecture, it is difficult to obtain high orientation of crystals for polypropylene random copolymers (PPR). In this work, two binary blends including polypropylene (PP)/ultrahigh molecular weight polyethylene (UHMWPE) and polypropylene random copolymer (PPR)/UHMWPE were fabricated via solution blending and subsequent melt shear through mini-injection molding. It was found that highly-oriented crystalline structure forms under shear flow in both blend series. The tensile strength of PP blends increased from 38.3MPa to 43.8MPa while the PPR blends showed a more significant property enhancement and increased from 32.5MPa to 38.1MPa. Importantly, PPR shows an increased miscibility with UHMWPE in

comparison with PP due to the existence of ethylene segments. The tensile toughness of PPR samples was greatly maintained especially for blends with small addition of UHMWPE, which may be ascribed to the crack-suppression effect originated from well-dispersed UHMWPE domains (particle size $< 0.50 \mu\text{m}$) locked by the co-crystal structures between PPR segments and molecularly mixed PE chains.

Keywords: Mechanical property; polymer blending; phase morphology; crystal orientation.

INTRODUCTION

As a well-known commercial plastic, isotactic polypropylene (iPP) gains substantial market shares and extensive applications such as packaging, automobile, functional components like battery separators due to its good processability, low cost and excellent chemical resistance [1-4]. Polypropylene(PP) is a semi-crystalline polymer whose molecular chains can self-organize into different crystalline polymorphs including α , β and γ phases [5-7]. Different phase morphologies endow PP good adaptability in various working conditions. However, in some engineering cases, the poor toughness at low temperature or under high strain rate limits its use. Polypropylene random copolymer (PPR) is synthesized by inserting 1-olefins such as ethylene, 1-butene, and 1-hexene into the PP chains, which improves the toughness to some extent [8,9]. But the high viscosity and elasticity induced by high molecular weight and broad molecular weight distribution restricted its processability. Meanwhile, the random insertion of a small amount of 1-olefin along the PP chains promotes the formation of short blocks and leads to lower crystallization temperature and overall crystallinity [8,10,11]. In all cases, it is fundamental and crucial for these PP-based materials to improve their mechanical properties to meet versatile requirements.

Extensive studies have been conducted to achieve targeted improvement in the mechanical properties of PP and copolymers. It is widely accepted that fabrication of PP-based composites or nanocomposites is one effective way [12-14]. Incorporating nanofillers into polypropylene (PP) can significantly reduce the weight of load-bearing components, enhancing their performance without compromising structural integrity. Glass-fiber reinforced PP composites exhibit advanced properties and can be easily processed through conventional methods like injection molding [15]. Similarly, layered silicates such as montmorillonite were added into PP system and dispersed into single layers

with the aid of interfacial compatibilization [16]. In recent years, carbon nanofillers is widely used in PP nanocomposites including carbon fiber, carbon nanotubes(CNT), and graphene [17-19]. The incorporation of nanofillers into polypropylene (PP) nanocomposites naturally endows them with novel functionalities, expanding their range of applications and performance capabilities [20]. For instance, Wu *et al.* used in-situ synthesis method to synthesize nano-silver and fabricate PP-based composites with good antibacterial property for disinfection purpose [21]. Thomassin *et al.* introduced carbon nanotube with a low concentration into polypropylene matrix with the purpose of effective electromagnetic interference (EMI) absorber [22]. Rubsam *et al.* developed an anchor-peptide-based toolbox for green polypropylene functionalization and further equipped polypropylene with the fluorescent dye via taking the anchored peptide as the adhesion promoter [23]. However, the filler-reinforced system inevitably faces challenges such as achieving a uniform dispersion of nanofillers within the matrix and scaling up the production of new types of nanofillers with superior physical properties.

Polymer blending is another versatile, low-cost and high-efficient method in polymer processing industry. Blending modified polypropylene (PP) with polyethylene (PE) is a widely adopted strategy in the polyolefin system. This approach is favored due to the similar chemical structures of the polymers, which allows for adjustable melt miscibility based on the topological chain structures of PE [24]. It was reported that linear low-density polyethylene (LLDPE) can possess a good miscibility with PP in a proper composition range while phase separation occurs when PP is blending with high-density polyethylene (HDPE) or low-density polyethylene (LDPE) [25]. In addition, coupling with external flow field always favors crystal orientation and high mechanical properties for polyolefin blends [26-28]. Fu and coworkers found that melt-drawing PP/HDPE blends upon cooling can direct lamellar orientation of PE by epitaxial crystallization especially when interfacial nucleation dominates [29]. For comparison, Fu et.al also investigated flow-induced epitaxial growth of HDPE in its blends with the low crystallizable PPR [30]. They found that epitaxy growth of PE on PPR crystal can be achieved in blends with 30wt%PE during shear condition while the epitaxy growth is hindered by the formation of shish-kebab when PE content is large [30]. In addition, previous reports clearly showed that small change of crystal structures and crystal morphology could alter the final mechanical performance [31]. In addition to conventional polyethylenes (PEs), ultrahigh molecular weight polyethylene (UHMWPE), known for its exceptional properties including superior wear resistance,

creep resistance, and high-impact strength, can be effectively integrated into PP-based systems to enhance their performance. Hashimi and coworkers investigated the effect of blend composition on sliding wear property of PP/UHMWPE blends and found that wear loss was significantly lower than that of PP due to improved temperature reduction at the contact surface [32]. Furthermore, Chen *et al.* constructed β -crystals in PP by adding UHMWPE combined with applying melt flow by microinjection molding machine [33]. Kamayar *et al.* explores the toughening mechanisms in polypropylene to achieve a balance between strength and toughness in thermoplastic composites [34]. Ding *et al.* reported the annealing effect on low-temperature toughness of PPR blends [35]. However, melt-blending cause phase separation and resulted in UHMWPE domain with several hundred micrometers within PP matrix. And it still remains to be addressed to effectively tune the crystalline morphology of PPR by adding UHMWPE since partial ethylene component in PPR may be favorable for the melt miscibility between PPR and UHMWPE.

In this work, we have prepared PP/UHMWPE and PPR/UHMWPE blends with the aid of solution-blending in consideration of possible molecular mixing. In order to exert melt shear and induce possible highly orientated crystals, both blend systems were prepared through mini-injection molding technique. The goal of this paper is to explore the effect of long chains of PE on the crystalline structures and final mechanical properties of PP and PPR system in which the intrinsic crystallization is different due to the insertion of co-monomers. As a consequence, PE long chains are favorable for tuning mechanical strength-toughness balance of PP or PPR systems especially under melt shear conditions mainly due to the formation of highly-oriented crystalline structures. This work provides some guidance for structure manipulation and optimizing mechanical property of polypropylene random copolymers.

EXPERIMENTAL

Materials

Polypropylene (PP) with a tradename of T30S was purchased from Dushanzi Petroleum Chemical Incorporation (Xinjiang, China), with a melt flow index of 0.96g/10min(190°C, 2.16kg). Polypropylene random copolymer (PPR) used in this study was purchased from Hyosun Company(Korea) with a tradename of R200P. The MFI index of PPR is 0.23 g/10min. It possesses a molecular weight of 720,000 g/mol and a PDI index of 4.5. The mass percentage of ethylene

component was as low as 3.8wt%. Ultrahigh molecular weight polyethylene (UHMWPE) powder was purchased from Second Auxiliary Factory (Beijing, China), with a molecular weight of 5,500,000 g/mol.

Sample preparation

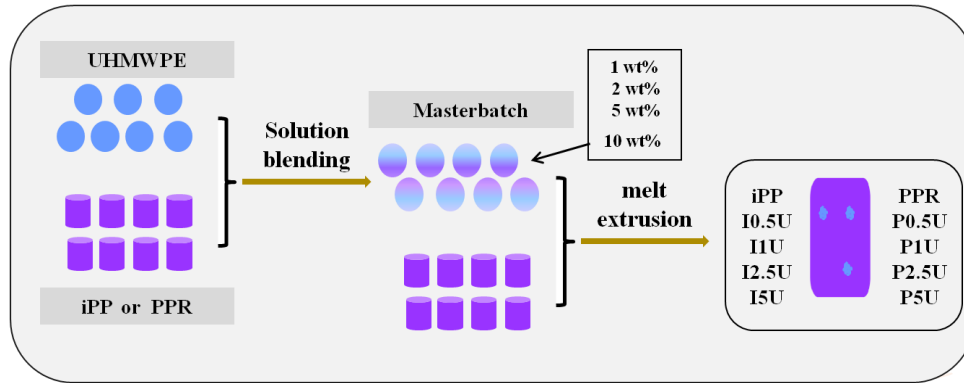


Figure 1. Schematic presentation for the preparation of IU and PU samples.

Figure 1 shows the schematic illustration for the preparation of PP and PPR samples blended with ultrahigh molecular weight polyethylene (UHMWPE). Firstly, a fixed content of UHMWPE was solution blended with iPP or PPR in hot xylene in order to achieve a molecularly mixed blend system. The above polymer blend was taken as a master batch. Then the master batch was melt blended with iPP or PPR pellets in a twin-screw extruder to produce iPP or PPR based samples containing different content of UHMWPE. A small amount of antioxidant (Irganox 1010) was added into the blends to prevent thermal decomposition during melt processing. In addition, the processing condition was set as processing temperature of 160-190°C from hopper to die with a fixed speed of 80 rpm. Finally, the blended samples were prepared by mini-injection molding, which can apply shearing on the melt. For simplicity, the iPP/UHMWPE blends were named as IxU while the PPR/UHMWPE blends were named as PxU, where x presents the content of UHMWPE. For example, P2.5U represents PPR sample containing 2.5 wt% UHMWPE.

Testing and characterization

A Perkin-Elmer diamond-II differential scanning calorimetry (DSC) was used to evaluate the crystallization and melting behaviors of PP/UHMWPE and PPR/UHMWPE blended samples. The cooling and heating rate was fixed as 10°C/min. The samples with a fixed weight of ~5mg were heating

first to erase thermal history and the cooling and subsequent second heating curves were recorded to evaluate the crystallization and melting behaviors of the blends.

Standard tensile tests were conducted on dumbbell-shaped samples using a SANS Universal tensile testing machine according to the ASTM D638-03 standard. The tensile speed was fixed as 50mm/min. The crystalline morphologies were evaluated by using a Hitachi S3400 scanning electron microscopy (SEM) with an acceleration voltage of 20kV. The samples were cryo-disrupted and the fracture surface was chemically etched by etching acids. Then the surface was sputtered by a thin layer of gold before observation.

Polarized Light Microscopy (PLM) equipped with a Linkam Hot stage (THMS-600) was used to capture morphological changes during predetermined thermal history. The extruded granules were melted at 190°C and squeezed to get thin films. Thin films were heated to 190°C for 5min again to erase thermal history and then the crystalline morphologies were recorded with camera during cooling. The injection-molded samples were tested by 2D-WAXD (Bruke DISCOVER d8 diffractometer). 1D azimuthal scans as a function of 2theta can be obtained by integration. Then the relative degree of crystallinity (X_c) can be calculated from the ratio of the area of crystalline peaks (A_c) to the whole area ($A=A_c+A_a$), where A_a is the area of amorphous halo.

$$X_c = A_c / (A_c + A_a) \quad (1)$$

The crystal orientation degree (f) can be quantitatively assessed by Herman's orientation factor [36-37]:

$$f = (3 \langle \cos^2 \phi \rangle - 1) / 2 \quad (2)$$

$$\langle \cos^2 \phi \rangle = \frac{\int_0^{\pi/2} I(\phi) \sin \phi \cos^2 \phi d\phi}{\int_0^{\pi/2} I(\phi) \sin \phi d\phi} \quad (3)$$

Where ϕ is the azimuthal angle and $\langle \cos^2 \phi \rangle$ indicates the average of $\cos^2 \phi$, $I(\phi)$ stands for the scattered intensity.

RESULTS AND DISCUSSION

The melt-miscibility and crystallization behavior of PP/UHMWPE and PPR/UHMWPE blends

Representative SEM micrographs obtained from iPP/U and PPR/U blend containing different content

of UHMWPE are presented in Figure 2. The inclusion of a mere 1wt% of ultrahigh molecular weight polyethylene (UHMWPE) demonstrates melt miscibility with isotactic polypropylene (iPP) and polypropylene rubber (PPR), as indicated by the absence of any segregated domain structures in Figures 2a and 2b. Wong *et al.* reported PP/PE blend generally show heterogeneous phase structure due to phase separation [38]. Our previous study on blending UHMWPE with olefin block copolymer presented that macrophase separation occurs for samples obtained simply by melt blending though the addition of UHMWPE is small [31]. Herein, solution blending is favorable for the melt miscibility because of the effective disentanglement of UHMWPE. Wang *et al.* also reported similar behavior for iPP/UHMWPE blends obtained by solution blending [39]. When the content of UHMWPE increases to 5wt%, both I5U and P5U shows a macrophase separated structure. I5U has dispersed UHMWPE phase domain with several microns up to about 5 μm in diameter. On the other hand, PPR shows an increased melt miscibility with UHMWPE compared with iPP with the same addition of UHMWPE. The phase domain of UHMWPE in PPR can remain a smaller size and narrower distribution. Furthermore, it can be seen that small UHMWPE particle located in the center of spherulites for both iPP and PPR, indicating an effective nucleating effect.

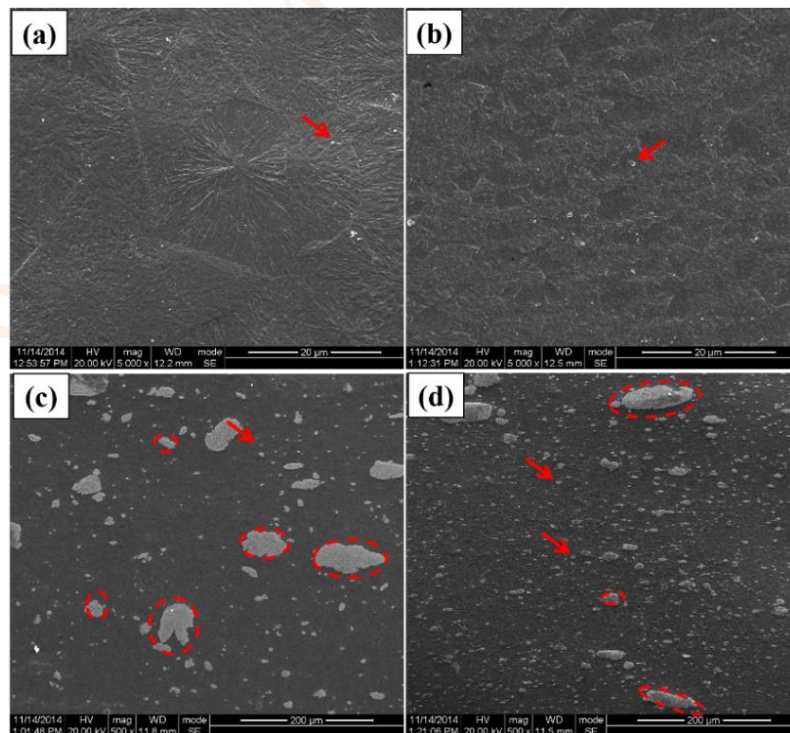


Figure 2. Typical SEM images of quenched samples of (a). I1U; (b). P1U; (c). I5U and (d). P5U.

Figure 3 presents the non-isothermal crystallization kinetics of iPP and PPR containing different content of UHMWPE. Fig. 3a and Fig. 3c shows the DSC curves for iPP/UHMWPE blends during cooling and subsequent heating scans with a fixed rate of 10°C/min. For the neat iPP, the onset crystallization temperature is 122.0°C and the crystallization peak temperature is 114.1°C. When iPP is blended with small amount of UHMWPE, there is still one single crystallization peak. With increasing the UHMWPE content, the crystallization peak gradually becomes sharp and the peak temperature ($T_{c,peak}$) increases, indicating UHMWPE plays a role of nucleating site. For I5U sample, the $T_{c,peak}$ even reaches 115.3°C, meaning gradual approaching to $T_{c,peak}$ of UHMWPE(117.6°C). Correspondingly, the melting curves of iPP/UHMWPE blended samples show one single melting peak though the peak melting behavior of pure UHMWPE occurs at 131°C. Consistent with previous findings, iPP initiates its crystallization process subsequent to the completion of the crystallization of UHMWPE [40]. UHMWPE crystals enhance the heterogeneous nucleation for iPP. Due to the close crystallization temperature, the crystallization peaks of these two components have overlapped into one single exothermic peak. In comparison, PPR possesses a $T_{c,peak}$ of ~100.1°C, which is ~10°C lower than that of iPP. When adding UHMWPE, $T_{c,peak}$ of PPR increases obviously from 101.7°C for P0.5U to 106.2°C for P5U, which further demonstrate an effective nucleating effect of UHMWPE in PPR melt. The pronounced nucleation effect imparted by the incorporation of UHMWPE significantly accelerates the crystallization process of PPR, leading to a marked enhancement in the material's overall crystallization kinetics. In addition, two individual crystallization peaks arise when UHMWPE content is high, indicating phase separation occurred between UHMWPE and PPR. The similar chain structure of PPR segment and UHMWPE is effective for miscibility and favors for the formation of co-crystal structure. Consequently, the melting curve also shows two peaks especially at high addition of UHMWPE, namely, an obvious two-step crystallization process. Overall, the result indicates that PPR shows higher melt miscibility with UHMWPE and a small portion of UHMWPE shows better nucleating effect in PPR relative to iPP system.

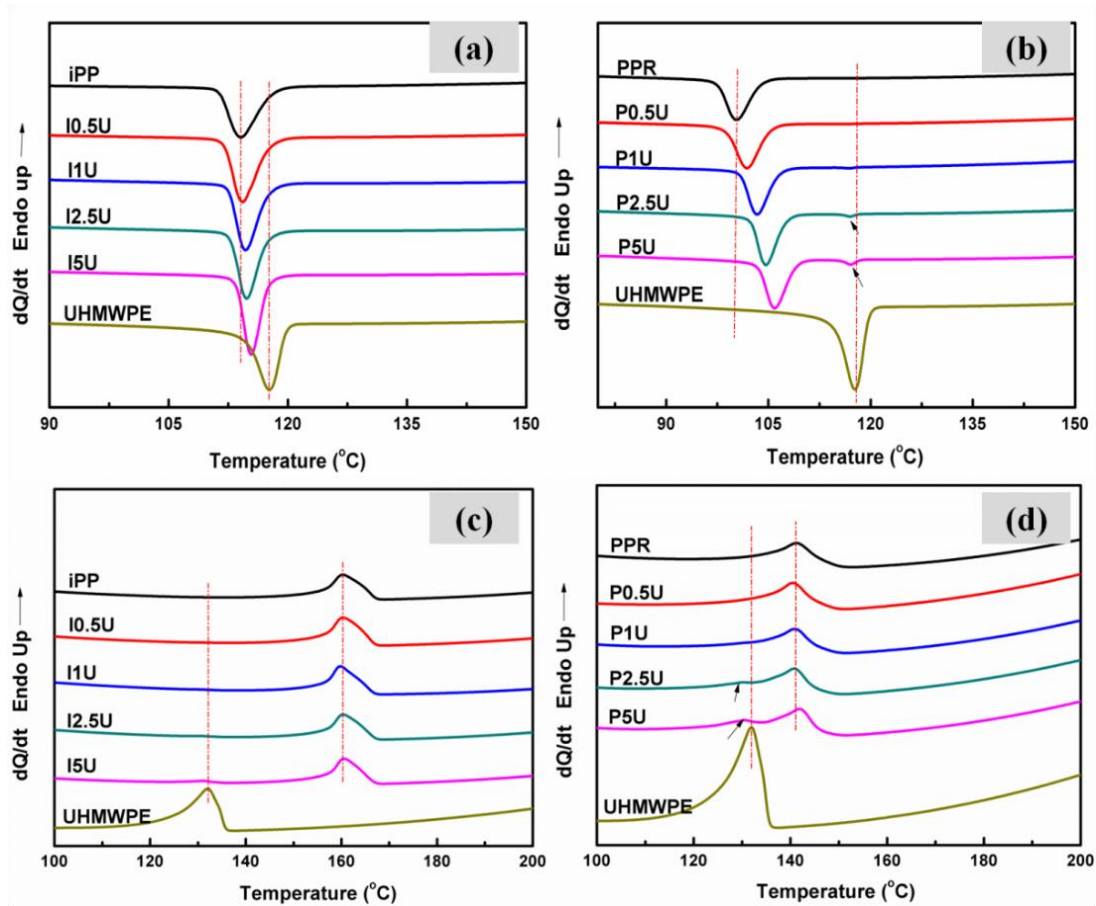


Figure 3. DSC curves of iPP/UHMWPE and PPR/UHMWPE blends with different UHMWPE content: (a). cooling scans for IU samples; (b). cooling scans for PU samples; (c). second heating scans for IU samples; (d). second heating scans for PU samples.

To further detect the two-step crystallization behavior of PPR/UHMWPE with high content of UHMWPE, selected POM images were captured at different stages under a temperature-jump (T-jump) treatment process. The detailed temperature-time protocol, which covers two isothermal stages correlated with two crystalline species, can be seen in Figure 4a. For pure PPR, there is no obvious crystal nuclei formed after crystallizing under 121°C for 10 min (Fig.4b1). Subsequently, further isothermal crystallization was conducted under 116°C and the evolution of crystalline morphologies was captured at different time. At early stage (1min at 116°C), there are several nuclei formed. As time progresses, the existing nuclei gradually increase in size, eventually reaching spherulite dimensions of approximately 150 μ m after isothermal crystallization for 5 minutes. At the same time, there are some new nuclei formed between different spherulites. As for PPR/UHMPWE, significant difference appears in terms of the crystallization kinetics and the crystalline morphology. As for P5R blend, in regardless of some phase-separated domain of UHMWPE due to limited miscibility, there are some

small nuclei formed even when isothermally crystallized under 121°C for 0.5 min. These nuclei is ascribed to UHMWPE which can be deduced from non-isothermal DSC data (Fig.3b). Comparatively, after T-jump treatment to 116°C, a large number of nuclei and small crystals formed in P5R blend when isothermally crystallized for 0.5min. With time evolution (2min at 116°C), close-connected spherulites formed and the crystal size greatly decreased to $\sim 15\mu\text{m}$, which also indicates the remarkable nucleation ability of UHMWPE. It is also easy to find out that the existence of UHMWPE gives rise to a much higher crystallization rate. The crystals even impinge with each other which is mainly accounted for the fast total crystallization rate during isothermal crystallization process. Therefore, large dispersed spherulites are observed in neat PPR sample while small and close-connected PPR spherulites formed in PPR/UHMWPE blends.

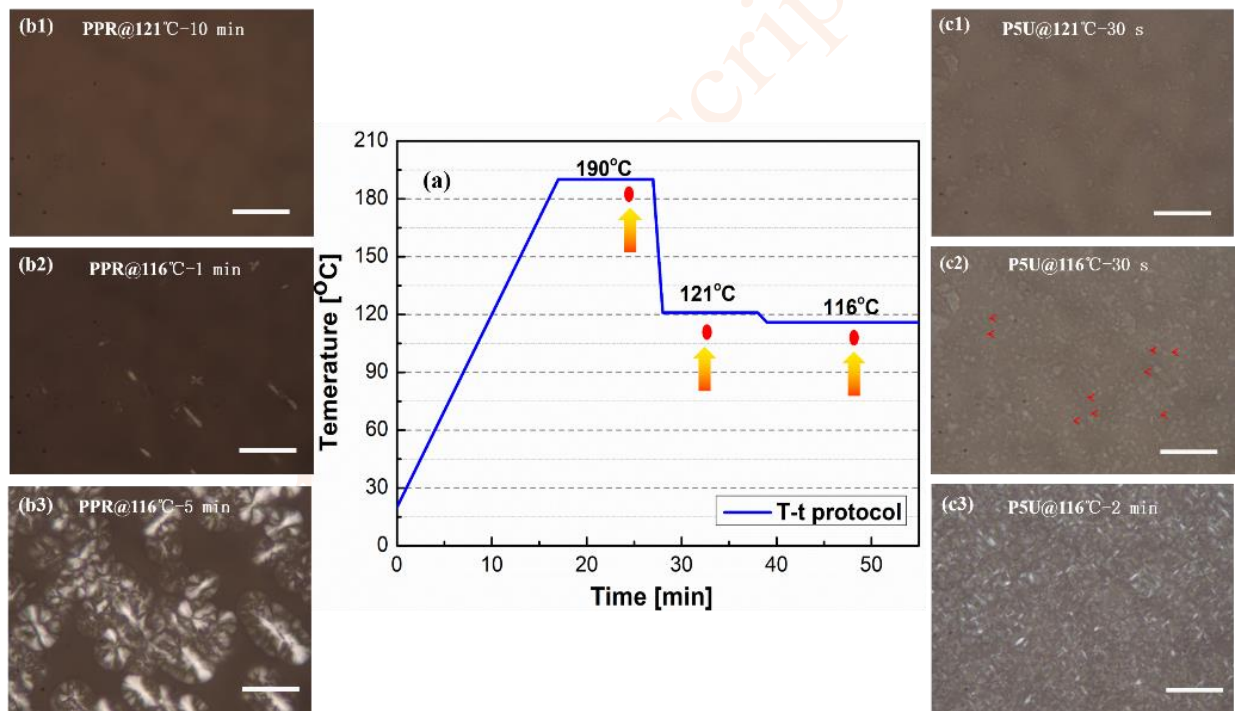


Figure 4. (a) Demonstration of the temperature-time protocol of thermal treatment; (b1-b3). typical POM images for PPR sample captured at different stage; (c1-c3). POM images for P5U sample captured at different stage. Note: the scale bar is 200 μm .

The crystalline morphology of PP/UHMWPE and PPR/UHMWPE samples

Despite of the quiescent crystallization behavior, crystalline morphologies under process conditions can determine the final mechanical performance of polymer samples. Consequently, the impact of melt shear on the crystalline structures was meticulously examined through the analysis of the

microstructure of samples produced via mini-injection molding. Fig.5a-c shows 2D WAXD patterns of I-U blends containing different content of UHMWPE. The flow direction was horizontal. The characteristic Debye rings located at different site mainly including (110), (040), and (111)/(-131) planes of PP. The (110) plane of PE crystals is overlapped with (111)/(-131) plane of PP crystal. It can be observed that the diffraction patterns of the samples presented sharp arcs, indicating strong orientation of the molecular chains in these samples. After the addition of UHMWPE, the diffraction arc of (040) in the blends becomes sharper than that of pure iPP, which indicates enhanced molecular orientation of iPP. As shown in Fig.5e, the overall crystallinity of I-U samples is nearly the same (~53%). In order to quantitatively analyze the crystal orientation level of different samples, (040) lattice planes of PP was selected to calculate orientation parameter. In Fig.5f. The calculated orientation degree was shown in Fig.5g. For pristine iPP, the degree of orientation reaches as high as 0.78, indicating a high molecular orientation. When adding small amount of UHMWPE, the degree of orientation (f) gradually increases with the increase of UHMWPE content. The results indicate that melt shear significantly promotes the formation of oriented structures, particularly in melts containing UHMWPE. This phenomenon is primarily attributed to the slow relaxation dynamics characteristic of UHMWPE. Therefore, the addition of UHMWPE is favorable for crystal orientation of iPP system.

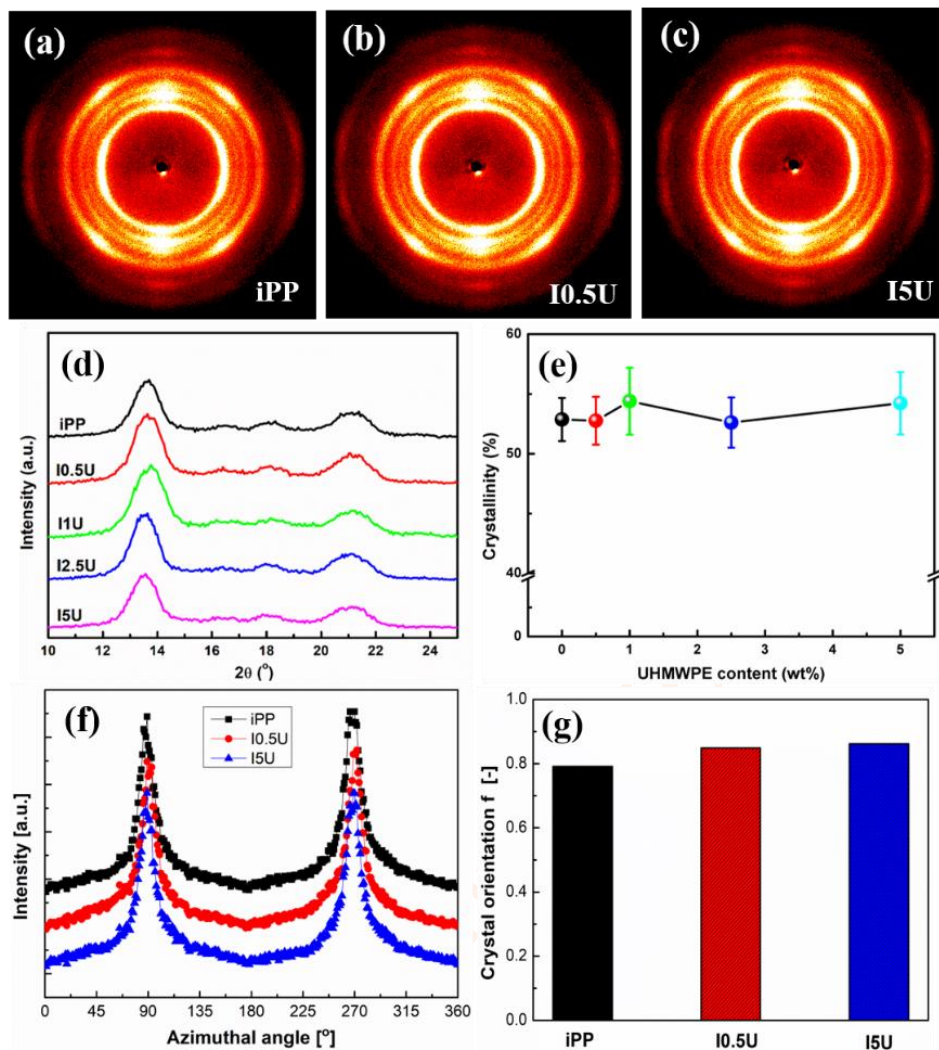


Figure 5. Typical 2D-WAXD patterns of iPP-U injection-molded samples: (a). iPP; (b). I0.5U; (c). I5U; (d). circularly averaged 1D-WAXD curves as a function of 2θ; (e). calculated overall crystallinity (X_c) as a function of UHMWPE content; (f). azimuthal scan intensities at (040) crystal plane; (g). the degree of crystal orientation (f) of three selected I-U samples. Note: the flow direction (FD) is horizontal.

For comparison, crystalline structure and crystal orientation were also evaluated on PPR/UHMWPE blends. Fig.6a-c shows 2D-WAXD patterns of PPR, P0.5U, P1U, respectively. Fig.6a-c shows 2D WAXD patterns of P-U blends containing different content of UHMWPE. The flow direction was horizontal. As for PPR system, α -crystal is also the typical crystal form. Similar to PP system, the characteristic diffraction arcs appeared at (110), (040), and (111)/(-131) planes. The short arc instead of circles indicated crystal orientation of PPR mainly induced by melt shear. After blending with UHMWPE, The orthogonal crystal form of PE possesses typical (110) and (020) crystal plane, which are overlapped with (111)/(-131) plane of PPR crystal. The diffraction arc corresponding to the (040) plane in the P-U samples exhibits progressive sharpening as the UHMWPE content increases, thereby

indicating a significant enhancement in crystal orientation. Fig.6e showed that the total crystallinity of P-U samples reaches ~ 0.53 and is nearly identical for P-U samples with different content of UHMWPE. Further quantitative analysis on the degree of crystal orientation was also conducted for P-U samples. As shown in Fig.6, the degree of orientation (f) of P-U samples gradually increased from 0.73 to 0.81 with the increase of UHMWPE content. Consequently, the incorporation of UHMWPE into PPR has successfully resulted in the attainment of a high degree of crystal orientation, underscoring the significant influence of UHMWPE on the crystallization behavior of the polymer matrix. It can be concluded that well-miscible UHMWPE within PPR melts effectively induce oriented crystalline structure for PPR during cooling which is good for property enhancement.

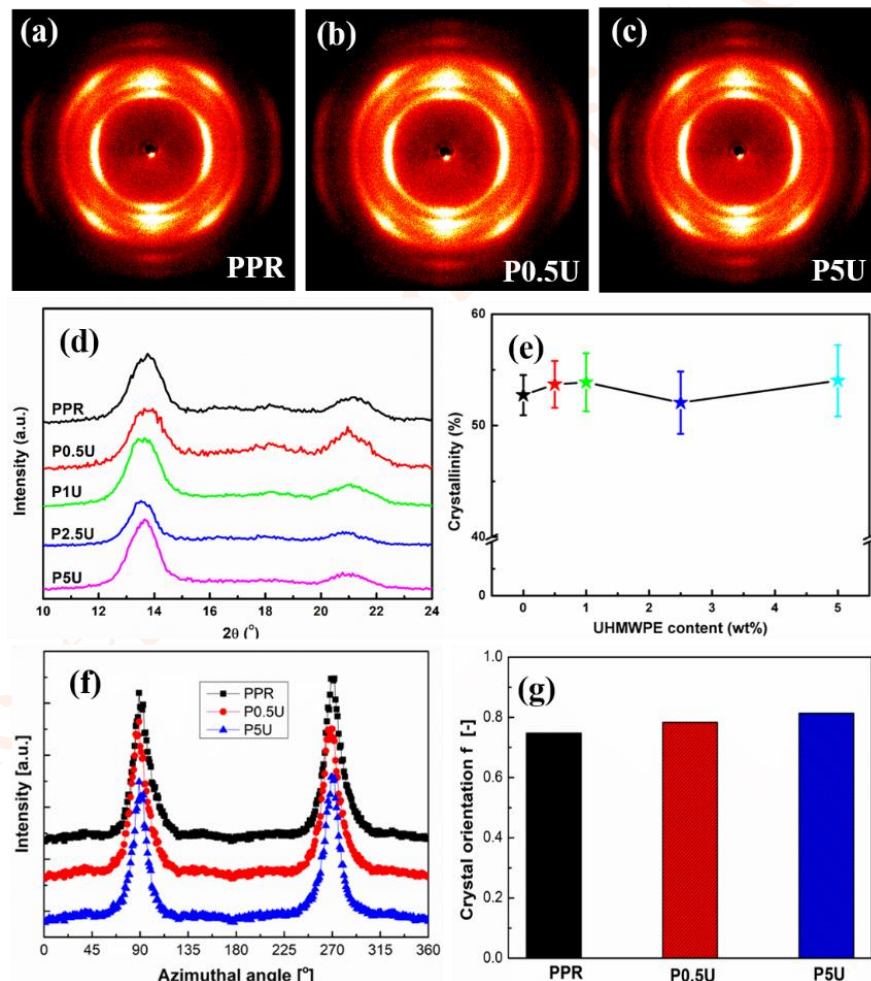


Figure 6. Typical 2D-WAXD patterns of PPR-U injection-molded samples: (a). PPR; (b). P0.5U; (c).P5U; (d). circularly averaged 1d-WAXD curves as a function of 2θ ; (e). calculated overall crystallinity(X_c) as a function of UHMWPE content; (f). azimuthal scan intensities at (040) crystal plane; (g). the degree of crystal orientation (f) of three selected P-U samples. Note: the flow direction (FD) is horizontal.

The mechanical properties of PP/UHMWPE and PPR/UHMWPE samples

Figure 7 presents the tensile stress-strain curves at room temperature for iPP/UHMWPE and PPR/UHMWPE blends. In the case of the iPP series, a characteristic ductile plastic fracture behavior is observed, which is manifested by yield deformation, followed by a substantial strain at break, accompanied by a slight strain-hardening effect. These findings are in accordance with prior research [41]. The yield stress of neat iPP is 38.3MPa. With the increasing addition of UHMWPE, the yield stress gradually increased to 43.8MPa, meaning ~14.4% property enhancement. At the same time, the elongation at break values of neat iPP reaches ~900%, indicating a good ductility. For iPP containing different content of UHMWPE, the elongation at break remains to a high level (>650%). On the other hand, the yield stress of neat PPR is 32.5MPa and the elongation at break is ~310%. With the increasing addition of UHMWPE, the yield stress of PPR/U blended samples significantly increase by ~47.7% to reach 38.1MPa, which is nearly comparative with I5U sample. Interestingly, I0.5U shows an increased tensile strength (~45.2MPa) and also presents an elongation at break of ~600%, indicating a two-fold increase of tensile toughness. Accordingly, the incorporation of UHMWPE significantly augments the properties of iPP and PPR, particularly by facilitating the development of oriented crystal structures. In addition, a simultaneous reinforcing and toughening effect was obtained for PPR/UHMWPE blends mainly due to the existence of partial PE segments in PPR molecular chains. For neat PP sample, tensile deformation can result in cavitation and the deformation of PP after yielding is generally inhomogeneous. After adding 1wt% UHMWPE, aligned fibrils can decrease the number of voids. Further adding UHMWPE to 5wt%, UHMWPE aggregated is dominating. The weak interfacial interaction between the PP and UHMWPE phases results in increased susceptibility to debonding and a reduction in elongation at break. In contrast, for PPR, the partial incorporation of ethylene monomers is beneficial for enhancing toughness. Because of the chain similarity between PE chains and PPR segments, molecularly mixed chains may form co-crystals and thus locking the phase-separated UHMWPE domains into smaller size. When P1U sample is stretched, UHMWPE domains can suppress crack propagation.

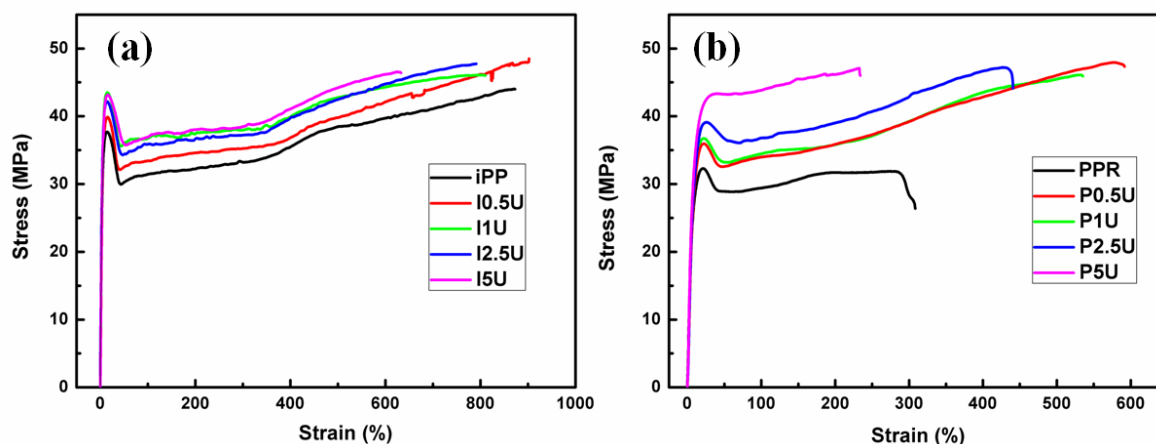


Figure 7. Tensile stress-strain curves of (a). iPP/UHMWPE and (b). PPR/UHMWPE blended samples.

CONCLUSIONS

In summary, the crystalline morphology and mechanical property of iPP and PPR filled with small amount of UHMWPE were investigated. For two blend series, low addition of UHMWPE is inclined to be miscible with the matrix while phase separation occurs at high addition of UHMWPE. When applied shear flow via mini-injection molding, both PP and PPR blends can achieve high crystal orientation, which is favorable for enhancement of mechanical strength. Though two-step crystallization process was observed for PPR/U blends, molecularly mixed chains may form co-crystals and thus locking the phase-separated UHMWPE domains into smaller size owing to the chain similarity between PE chains and PPR segments. In this way, crack suppressing effect from UHMWPE particles give rise to a simultaneous enhancement of tensile toughness for PPR/U blends. As a consequence, PPR systems showed a balanced mechanical stiffness and toughness. This work shows a simple and effective approach to realize morphological control and tune mechanical property in PPR via blending with UHMWPE.

ACKNOWLEDGEMENT

The authors gratefully thank the financial support from the Third Batch of Science and Technology Project of Qinghai Province in 2022 (Qingke Development Regulation [2022] No. 84).

REFERENCES

1. Guo Q, Li X, Li W, Yao Z (2018) The balanced insulating performance and mechanical property of PP by

- introducing PP-g-PS graft copolymer and SEBS elastomer. *Ind Eng Chem Res* 57: 6696–6704 [\[CrossRef\]](#)
2. Phua SL, Yang L, Toh CL, Guoqiang D, Lau SK, Dasari A, Lu X (2013) Simultaneous enhancements of UV resistance and mechanical properties of polypropylene by incorporation of dopamine-modified clay. *ACS Appl Mater Int* 5: 1302-1309 [\[CrossRef\]](#)
 3. Morlat S, Maillhot B, Gonzalez D, Gardette JL (2004) Photo-oxidation of polypropylene/montmorillonite nanocomposites. 1. Influence of nanoclay and compatibilizing agent. *Chemistry of materials* 16: 377-383 [\[CrossRef\]](#)
 4. Liu YM, Tong ZZ, Huang J, Zhou B, Xu JT, Fu ZS, Fan ZQ (2013) Regulation of phase separation in PP/EPR in-reactor alloy and its effect on crystallization kinetics. *Ind Eng Chem Res* 52: 16239-16246 [\[CrossRef\]](#)
 5. Luo F, Zhu Y, Wang K, Deng H, Chen F, Zhang Q, Fu Q (2012) Enhancement of β -nucleated crystallization in polypropylene random copolymer via adding isotactic polypropylene. *Polymer* 53: 4861-4870 [\[CrossRef\]](#)
 6. Zhu Y, Zhao Y, Fu Q (2016) Toward uniform pore-size distribution and high porosity of isotactic polypropylene microporous membrane by adding a small amount of ultrafine full-vulcanized powder rubber. *Polymer* 103: 405-414 [\[CrossRef\]](#)
 7. Fan J, Feng J (2013) Study on β -nucleated controlled-rheological polypropylene random copolymer: crystallization behavior and a possible degradation mechanism. *Ind Eng Chem Res* 52: 761-770 [\[CrossRef\]](#)
 8. Wang B, Chen Z, Kang J, Yang F, Chen J, Cao Y, Xiang M (2015) Influence of melt structure on the crystallization behavior and polymorphic composition of polypropylene random copolymer. *Thermochim Acta* 604: 67-76 [\[CrossRef\]](#)
 9. Ren Q, Fan J, Zhang Q, Yi J, Feng J (2016) Toughened polypropylene random copolymer with olefin block copolymer. *Mate Des* 107: 295-301 [\[CrossRef\]](#)
 10. Cao J, Lü QF (2011) Crystalline structure, morphology and mechanical properties of β -nucleated controlled-rheology polypropylene random copolymers. *Polym Test* 30: 899-906 [\[CrossRef\]](#)
 11. Cao J, Zheng Y, Lin T (2016) Synergistic toughening effect of β -nucleating agent and long chain branching on polypropylene random copolymer. *Polym Test* 55: 318-327 [\[CrossRef\]](#)
 12. Yuan W, Wang F, Chen Z, Gao C, Liu P, Ding Y, Zhang S, Yang M (2018) Efficient grafting of polypropylene onto silica nanoparticles and the properties of PP/PP-g-SiO₂ nanocomposites. *Polymer* 151: 242-249 [\[CrossRef\]](#)
 13. Cui L, Wang P, Zhang Y, Zhang L, Chen Y, Wang L, Liu L, Guo X (2017) Combined effect of α -nucleating agents and glass fiber reinforcement on a polypropylene composite: A balanced approach. *RSC Adv* 7: 42783-42791 [\[CrossRef\]](#)

14. Zhu Y, Zhao Y, Deng S, Zhang Q, Fu Q (2015) Largely enhanced mechanical properties and heat distortion temperature of β -nucleated isotactic polypropylene by adding ultrafine full-vulcanized powdered rubber. *RSC Adv* 5: 62797-62804 [\[CrossRef\]](#)
15. Lohr C, Dieterle S, Menrath A, Weidenmann KA, Elsner P (2018) Rheological studies on gas-laden and long glass fiber reinforced polypropylene through an inline high pressure capillary rheometer in the injection molding process. *Polym Test* 71: 27-31 [\[CrossRef\]](#)
16. Stribeck N, Zeinolebadi A, Ganjaee Sari M, Botta S, Jankova K, Hvilsted S, Drozdov A, Klitkou R, Potarniche CG, Christiansen JD, Ermini V (2012) Properties and Semicrystalline Structure Evolution of Polypropylene. *Macromolecules* 45: 962-973 [\[CrossRef\]](#)
17. Zhang K, Li Y, He X, Nie M, Wang Q (2018) Mechanical interlock effect between polypropylene/carbon fiber composite generated by interfacial branched fibers. *Compos Sci Technol* 167: 1-6 [\[CrossRef\]](#)
18. Yuan B, Bao C, Song L, Hong N, Liew KM, Hu Y (2014) Preparation of functionalized graphene oxide/polypropylene nanocomposite with significantly improved thermal stability and studies on the crystallization behavior and mechanical properties. *Chem Eng J* 237: 411-420 [\[CrossRef\]](#)
19. Yang H, Ye L, Gong J, Li M, Jiang Z, Wen X, Chen H, Tian N, Tang T (2017) Simultaneously improving the mechanical properties and flame retardancy of polypropylene using functionalized carbon nanotubes by covalently wrapping flame retardants followed by linking polypropylene. *Mater Chem Front* 1: 716-726 [\[CrossRef\]](#)
20. Masuda JI, Torkelson JM (2008) Dispersion and major property enhancements in polymer/multiwall carbon nanotube nanocomposites via solid-state shear pulverization followed by melt mixing. *Macromolecules* 41: 5974-5977 [\[CrossRef\]](#)
21. Wu JJ, Lee GJ, Chen YS, Hu TL (2012) The synthesis of nano-silver/polypropylene plastics for antibacterial application. *Curr Appl Phys* 12: S89-S95 [\[CrossRef\]](#)
22. Thomassin JM, Huynen I, Jerome R, Detrembleur C (2010) Functionalized polypropylenes as efficient dispersing agents for carbon nanotubes in a polypropylene matrix; application to electromagnetic interference (EMI) absorber materials. *Polymer* 51: 115-121 [\[CrossRef\]](#)
23. RübSam K, Stomps B, Böker A, Jakob F, Schwaneberg U (2017) Anchor peptides: A green and versatile method for polypropylene functionalization. *Polymer* 116: 124-132 [\[CrossRef\]](#)
24. Furukawa T, Sato H, Kita Y, Matsukawa K, Yamaguchi H, Ochiai S, Siesler HW, Ozaki Y (2006) Molecular structure, crystallinity and morphology of polyethylene/polypropylene blends studied by Raman mapping, scanning electron microscopy, wide angle X-ray diffraction, and differential scanning calorimetry. *Polym J* 38:

1127-1136 [\[CrossRef\]](#)

25. Dahal P, Kim JH, Kim YC (2014) Effects of linear low density polyethylene on physical properties and irradiation effectiveness of polypropylene. *Korean J Chem Eng* 31: 1-5 [\[CrossRef\]](#)
26. Zhao Y, Zhu Y, Sui G, Chen F, Zhang Q, Fu Q (2015) The effect of hard block content on the orientation and mechanical properties of olefin block copolymer films as obtained via melt stretching. *RSC Adv* 5: 82535-82543 [\[CrossRef\]](#)
27. Zhao Y, Si L, Wang L, Dang W, Bao J, Lu Z, Zhang M (2017) Tuning the mechanical properties of weakly phase-separated olefin block copolymer by establishing co-crystallization structure with the aid of linear polyethylene: the dependence on molecular chain length. *CrystEngComm* 19: 2884-2893 [\[CrossRef\]](#)
28. Zhao Y, Liu Z, Su B, Chen F, Fu Q, Ning N, Tian M (2015) Property enhancement of PP-EPDM thermoplastic vulcanizates via shear-induced break-up of nano-rubber aggregates and molecular orientation of the matrix. *Polymer* 20: 170-178 [\[CrossRef\]](#)
29. Na B, Wang K, Zhao P, Zhang Q, Du R, Fu Q, Yu Z, Chen E (2005) Epitaxy growth and directed crystallization of high-density polyethylene in the oriented blends with isotactic polypropylene. *Polymer* 46: 5258-5267 [\[CrossRef\]](#)
30. Su R, Li Z, Bai H, Wang K, Zhang Q, Fu Q, Zhang Z, Men Y (2011) Flow-induced epitaxial growth of high density polyethylene in its blends with low crystallizable polypropylene copolymer. *Polymer* 52: 3655-3660 [\[CrossRef\]](#)
31. Zhao Y, Zhu Y, Sui G, Chen F, Fu Q (2017) Tailoring the crystalline morphology and mechanical property of olefin block copolymer via blending with a small amount of UHMWPE. *Polymer* 109: 137-145 [\[CrossRef\]](#)
32. Hashmi SA, Neogi S, Pandey A, Chand N (2001) Sliding wear of PP/UHMWPE blends: effect of blend composition. *Wear* 247: 9-14 [\[CrossRef\]](#)
33. Chen Q, Xiang Z, Yang Q, Kong M, Huang Y, Liao X, Niu Y, Zhao Z (2016) Flow-induced β -crystal of iPP in microinjection molding: effects of addition of UHMWPE and the processing parameters. *J Polym Res* 23: 1-11 [\[CrossRef\]](#)
34. Shivanimoghaddam K, Balaji KV, Yadav R, Zabihi O, Ahamadi M, Adetunji P, Naebe M (2021) *Compos B-Eng* 223: 109121-109153 [\[CrossRef\]](#)
35. Ding HL, Guo LY, Li DJ, Zheng D, Chen J, Qian YY (2015) Effect of annealing temperature on low-temperature toughness of β -nucleated polypropylene random copolymer/ethylene-propylene-diene terpolymer blends. *Chin J Polym Sci* 33: 256-264 [\[CrossRef\]](#)
36. Somani RH, Hsiao BS, Nogales A, Fruitwala H, Srinivas S, Tsou AH (2001) Structure development during shear flow induced crystallization of i-PP: in situ wide-angle X-ray diffraction study. *Macromolecules* 34: 5902-5909

[\[CrossRef\]](#)

37. Marco Y, Chevalier L, Chaouche M (2002) WAXD study of induced crystallization and orientation in poly (ethylene terephthalate) during biaxial elongation. *Polymer* 43: 6569-6574 [\[CrossRef\]](#)
38. Wong AY, Lam F (2002) Study of selected thermal characteristics of polypropylene/polyethylene binary blends using DSC and TGA. *Polym Test* 21: 691-696 [\[CrossRef\]](#)
39. Shao W, Zhang Y, Wang Z, Niu Y, Yue R, Hu W (2012) Critical content of ultrahigh-molecular-weight polyethylene to induce the highest nucleation rate for isotactic polypropylene in blends. *Ind Eng Chem Res* 51: 15953-15961 [\[CrossRef\]](#)
40. Liu G, Chen Y, Li H (2004) Study on processing of ultrahigh molecular weight polyethylene/polypropylene blends. *J Appl Polym Sci* 94: 977-985 [\[CrossRef\]](#)
41. López-Barrón CR, Tsou AH (2017) Strain hardening of polyethylene/polypropylene blends via interfacial reinforcement with poly (ethylene-cb-propylene) comb block copolymers. *Macromolecules* 50: 2986–2995 [\[CrossRef\]](#)

Accepted Manuscript (POM)